J. Fluid Mech. (1983), *vol.* 132, *pp.* 163–183
Printed in Great Britain

A theory for flow separation

By WILLIAM S. VORUS

Department of Naval Architecture and Marine Enginering, The University of Michigan, Ann Arbor, Michigan 48109

(Received 27 September 1982)

This paper proposes a high-Reynolds-number theory for the approximate analysis of timewise steady viscous flows. Its distinguishing feature is linearity. But it differs fundamentally from Oseen's (1910) well-known linear theory. Oseen flow is a variation on Stokes flow at the low-Reynolds-number limit.

The theory is developed for a 2-dimensional body moving through an infinite incompressible fluid. The velocity–vorticity formulation is employed. A boundary integral expressing the body contour velocity is written in terms of Green functions of the approximate governing differential equations. The boundary integral contains three unknown boundary distributions. These are a velocity source density, the boundary vorticity, and the normal gradient of the boundary vorticity. The unknown distributions are determined as the solutions to a boundary-integral equation formed from the velocity integral by the prescription of zero relative fluid velocity on the body boundary.

The linear integral-equation formulation is applied specifically to the case of thin bodies, such that the boundary condition is satisfied approximately on the streamwise coordinate axis. The integral equation is then reduced to its leading-order contribution in the limit of infinite Reynolds number. The unknown distributions uncouple in the first-order formulation, and analytic solutions are obtained. A most interesting result appears at this point: the theory recovers linearized airfoil theory in the first-order infinite-Reynolds-number limit; the airfoil integral equation determines one of the three contour distributions sought.

The first-order theory is then demonstrated by application to two classical cases: the zero-thickness flat plate at zero incidence, and the circular cylinder.

For the flat plate, the streamwise velocity near the plate predicted by the proposed linear theory is compared with that of Blasius's solution to the laminar boundary-layer equations (Schlichting 1968). The linear theory predicts a fuller profile, tending more toward the character expected of the timewise steady turbulent profile. This character is also exhibited in the predicted velocity distribution across the plate wake, which is compared with Goldstein's asymptotic boundary-layer solution (Schlichting 1968). The wake defect is more severe according to the proposed theory.

For the case of the circular cylinder, application of the formulation is not truly valid, since the circular cylinder is not a thin body. The theory does, however, predict that the flow separates. The separation points are predicted to lie at position angles of approximately $\pm 135°$, with angle measured from the forward stagnation point. This compares with the prediction of 109° from the Blasius series solution to the laminar boundary-layer equations (Schlichting 1968).

The theory is next applied to the case of a non-zero-thickness flat plate with incidence. From the fully attached flow at zero incidence, the theory predicts that both leading-edge separation and reattachment and trailing-edge separation appear on the suction side at small angle. On increasing incidence, the forward reattachment

point moves aft, and the aft separation point moves forward. Coalescence occurs near midchord, and the foil is thereafter fully separated.

Finally, the first-order contribution to the far-field velocity at high Reynolds number is shown to be identically that corresponding to the ideal flow. This result, coupled with the recovery of linearized thin-foil theory in the near-field limit, is argued to support strongly the physical idea that the ideal flow is, in fact, the limiting state of the complete field flow at infinite Reynolds number. Flow separation can be viewed as present in the ideal flow limit; it is simply embedded in the infinitesimally thin body-surface vortex sheets into which the entire viscous field collapses as vorticity convection overwhelms vorticity diffusion at the infinite-Reynolds-number limit.

1. Introduction

Boundary-layer theory is a high-Reynolds-number approximation to the incompressible field equations which is not useful for the analysis of separated flows. The fault is believed to have its origins in the segregation of the viscous and ideal constituents of the complete flow into separate solution domains (Batchelor 1970).

A high-Reynolds-number approximation to the field equations different from boundary-layer theory is proposed here. Like boundary-layer theory, this new theory is approximate, but the approximations are different. The essential approximation is linearity. However, the treatment of the viscous and ideal constituents of the high-Reynolds-number flow is unified; the single solution domain is the complete field. The unified theory predicts the characteristics of separated flows completely, but, of course, approximately.

The proposed theory demonstrates other characteristics which are to the enhancement of its credibility. It recovers linear ideal-flow theory in the limit of infinite Reynolds number; thin airfoil theory, for example, appears in the limit. It predicts that, at high Re, positions of separation and reattachment points are independent of Reynolds number. In taking the limit to the ideal flow, the separation and reattachment points maintain position. The separated flow is predicted simply to collapse, along with all other viscous-flow characteristics, into the infinitesimally thin body-surface vortex sheets as diffusion time tends to zero relative to convection time at the infinite-Reynolds-number limit.

The theory is developed for the two-dimensional infinite-fluid case, but is applicable, in general, to more complex configurations.

2. Two-dimensional formulation

The theory is developed in terms of the 2-dimensional flow depicted on figure 1. Here, a general 2-dimensional body is fixed in a stream which has uniform velocity U in the positive x-direction at infinity. The fluid domain is the region denoted as S, bounded internally by the body-surface contour l_b and externally by the contour l_∞ of infinite radius.

It is assumed that the flow is time-independent, which excludes both turbulence and any unsteadiness of the shed laminar flow.

The velocity–vorticity formulation is employed. The three applicable differential equations are

$$\left.\begin{aligned} \boldsymbol{V}\cdot\boldsymbol{\nabla}\omega - \nu\nabla^2\omega = 0, \\ \boldsymbol{\nabla}\cdot\boldsymbol{V} = 0, \\ \boldsymbol{\nabla}\times\boldsymbol{V} = \omega\boldsymbol{k} \end{aligned}\right\} \quad \text{in } S \qquad \begin{aligned} &(1)\\ &(2)\\ &(3) \end{aligned}$$

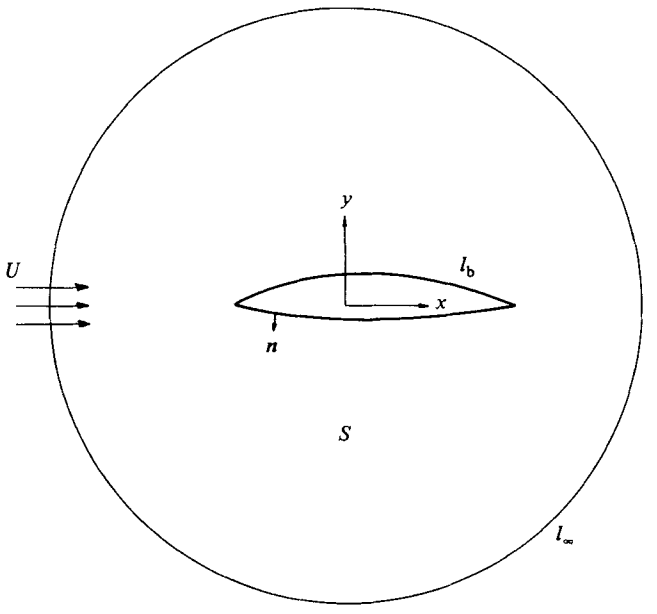

FIGURE 1. Flow configuration.

with boundary conditions

$$\left.\begin{aligned} \boldsymbol{V} &= 0, \\ \omega \boldsymbol{k} \cdot \boldsymbol{n} &= 0 \end{aligned}\right\} \quad \text{on } l_b, \tag{4, 5}$$

$$\left.\begin{aligned} \boldsymbol{V} &= U\boldsymbol{i}, \\ \omega &= 0 \end{aligned}\right\} \quad \text{on } l_\infty. \tag{6, 7}$$

The requirement (5) for vorticity tangency on the body-surface contour is satisfied identically in the 2-dimensional case, since $\boldsymbol{k} \cdot \boldsymbol{n} \equiv 0$.

The scheme proposed here for approximately solving the formulation (1)–(7) involves first inverting the differential equations (1) and (3), subject to (2), but independently of one another. That is, (3) is inverted as an integral expressing the field velocity in terms of the field vorticity, with continuity preserved. Equation (1) is then inverted as an integral expressing the field vorticity in terms of the field velocity, with continuity preserved. A key approximation is then made which allows the separate integrals to be combined as a boundary-integral equation, through which the problem boundary conditions can be satisfied. These steps are developed in the following.

2.1. *Inverse of* (3) *subject to* (2)

The inverse of $\boldsymbol{\omega} = \text{curl } \boldsymbol{V}$, subject to continuity, is well known for the infinite-fluid case. The homogeneous solution to (3), i.e. from $\nabla \times \boldsymbol{V}_h = 0$, is just the potential flow, obtained by solving (2) directly, in terms of a velocity potential:

$$\boldsymbol{V}_h = \boldsymbol{C} + \int_{l_b} \sigma \nabla G \, dl. \tag{8}$$

Here σ is an arbitrary source distribution on the body contour and G is the Green function of the potential-flow problem. In this case $G = (2\pi)^{-1} \ln r$. $\boldsymbol{C}$ in (8) is an arbitrary constant.

The complete solution to the non-homogeneous equation (3) is obtained by adding a particular solution, which also satisfies continuity. The complete solution, with $\boldsymbol{C} = U\boldsymbol{i}$, is

$$\boldsymbol{V} = U\boldsymbol{i} + \int_{l_b} \sigma \nabla G \, dl + \iint_S \omega \boldsymbol{k} \times \nabla G \, dS. \tag{9}$$

Here, with $G = (2\pi)^{-1} \ln r$, the particular solution is just the Biot–Savart law in terms of the unknown vorticity distribution. Note that the solution (9) satisfies the boundary condition (6), if ω satisfies (7).

2.2. *Inverse of* (1) *subject to* (2)

Here, a new Green function, for vorticity, denoted by g, is introduced. Henceforth g is referred to as the vorticity Green function, as against G, the velocity potential Green function.

The solution to (1) in terms of g is found in the usual way. First multiply (1) by g and integrate over the fluid region S. Then integrate that integral by parts to achieve the intermediate result

$$\iint_S [(\boldsymbol{V} \cdot \nabla \omega - \nu \nabla^2 \omega) g + (\boldsymbol{V} \cdot \nabla g + g \nabla \cdot \boldsymbol{V} + \nu \nabla^2 g) \omega] \, dS = \int_{l_b + l_\infty} \left[\nu \left(\omega \frac{\partial g}{\partial n} - g \frac{\partial \omega}{\partial n} \right) + \omega g (\boldsymbol{V} \cdot \boldsymbol{n}) \right] dl. \tag{10}$$

Substitute (1) and (2) into the left-hand side of (10), and recognize that (4) requires that $\boldsymbol{V} \cdot \boldsymbol{n} = 0$ on l_b. This reduces (10) to

$$\iint_S (\boldsymbol{V} \cdot \nabla g + \nu \nabla^2 g) \omega \, dS = \nu \int_{l_b + l_\infty} \left(\omega \frac{\partial g}{\partial n} - g \frac{\partial \omega}{\partial n} \right) dl + \int_{l_\infty} \omega g (\boldsymbol{V} \cdot \boldsymbol{n}) \, dl. \tag{11}$$

In view of (7), the integrals over l_∞ in (11) can be eliminated by requiring

$$g = 0 \quad \text{on } l_\infty. \tag{12}$$

Furthermore, in the interest of achieving $\omega(\boldsymbol{r})$ as the left-hand side of (11), require that g satisfy the differential equation,

$$\boldsymbol{V} \cdot \nabla g + \nu \nabla^2 g = \nu \delta(\boldsymbol{r} - \boldsymbol{r}_0). \tag{13}$$

Here $\boldsymbol{r}_0$ represents the variable of integration in (11), and $\boldsymbol{r}$, the field point vector in S, is the independent variable.

Substitute (12) and (13) into (11), with the result

$$\omega(\boldsymbol{r}) = \int_{l_b} \left(\omega \frac{\partial g}{\partial n} - \frac{\partial \omega}{\partial n} g \right) dl. \tag{14}$$

This integral represents the field vorticity in terms of its distribution and the distributions of its normal gradient on the body contour. The g required in (14) is the solution to the boundary-value problem defined by (12) and (13).

3. Linearization

The difficulty in going further with (14) lies in solving the differential equation (13). This is because its coefficient $\boldsymbol{V}$ is unknown. The essential feature of the proposed theory is approximation of $\boldsymbol{V}$ in (13) by a known function. This is the linearization of the problem to which all previous reference has been made.

The simplest and most obvious approximation of $\boldsymbol{V}$ for purposes of solving (12) and (13) is just the flow at infinity, $\boldsymbol{V} = U\boldsymbol{i}$. Adopting this approximation, the differential equation governing g is further simplified to a linear one with constant coefficients, and a relatively simple analytic solution is guaranteed.

From a physical point of view, replacing $\boldsymbol{V}$ by $U\boldsymbol{i}$ in (13) represents an approximation of vorticity convection relative to vorticity diffusion. In general, vorticity convection will be overestimated very near the body surface, and near the body stagnation points. It may be underestimated, on the average, in regions away from stagnation points and where flow separation is not occurring. The error should be least, in an overall sense, for streamlined bodies.

The approximation $\boldsymbol{V} = U\boldsymbol{i}$ in (13) should not necessarily preclude the prediction of separated flow, in spite of $U\boldsymbol{i}$ being a very poor approximation of the separation-flow velocity. For separation regions that are 'thin' enough relative to the thickness of the overall viscous-flow region, the net convection of vorticity would still be downstream, and with an average velocity of which $\boldsymbol{V} = U\boldsymbol{i}$ might not be a fatally severe approximation.

From a mathematical point of view, the accuracy of a boundary-value-problem solution is, in general, more sensitive to the accuracy employed in satisfying the problem boundary conditions than to the accuracy in the representation of the differential-equation coefficients. The boundary conditions (4)–(7) of the problem at hand are to be satisfied with conventionally accepted rigour.

4. The vorticity green function

With the approximation $\boldsymbol{V} = U\boldsymbol{i}$ in (13), the vorticity Green function is the solution to

$$U\frac{\partial g}{\partial x}+\nu\left(\frac{\partial^2 g}{\partial x^2}+\frac{\partial^2 g}{\partial y^2}\right)=\nu\delta(x-\xi)\,\delta(y-\eta) \quad (-\infty<x<\infty;\ -\infty<y<\infty), \tag{15}$$

with the boundary condition

$$g\to 0 \quad \text{as} \quad x^2+y^2\to\infty.$$

The x-wise Fourier transform of (15) produces

$$\left.\begin{aligned}\frac{\mathrm{d}^2 g^*}{\mathrm{d}y^2}-k\left(k-\frac{\mathrm{i}U}{\nu}\right)g^*=\mathrm{e}^{-\mathrm{i}k\xi}\,\delta(y-\eta) \quad (-\infty<y<\infty),\\ g^*\to 0 \quad \text{as} \quad |y|\to\infty,\end{aligned}\right\} \tag{16}$$

where $g^*(k, y; \xi, \eta)$ is the Fourier transform of $g(x, y; \xi, \eta)$.

The solution to (16) is

$$g^*=-\frac{1}{2}\frac{\mathrm{e}^{-\mathrm{i}k\xi}}{\left[k\left(k-\frac{\mathrm{i}U}{\nu}\right)\right]^{\frac{1}{2}}}\exp\left\{-\left[k\left(k-\frac{\mathrm{i}U}{\nu}\right)\right]^{\frac{1}{2}}|y-\eta|\right\},$$

with inverse

$$g=-\frac{1}{4\pi}\int_{k=-\infty}^{\infty}\frac{\exp\left\{-\left[k\left(k-\frac{\mathrm{i}U}{\nu}\right)\right]^{\frac{1}{2}}|y-\eta|\right\}}{\left[k\left(k-\frac{\mathrm{i}U}{\nu}\right)\right]^{\frac{1}{2}}}\mathrm{e}^{\mathrm{i}k(x-\xi)}\,\mathrm{d}k. \tag{17}$$

Here the interest in high Reynolds number can be exploited. If the body Reynolds number UL/ν is large, only small values of k contribute significantly to the integral in (17). Its first-order approximation in this case becomes

$$g \approx -\frac{1}{4\pi}\int_{k=-\infty}^{\infty} \frac{\exp\left[-\left(\frac{-ikU}{\nu}\right)^{\frac{1}{2}}|y-\eta|\right]}{\left(-\frac{ikU}{\nu}\right)^{\frac{1}{2}}} e^{ik(x-\xi)}\,dk. \tag{18}$$

The above reduction is equivalent to ignoring vorticity diffusion in the streamwise direction, which is a conventional approximation employed in high-*Re* viscous-flow analysis.

It is in fact at (18) that the proposed theory diverges away from Oseen's (1910) well-known linearization of the viscous field equations. Oseen's linearized theory was developed as an improvement on Stokes flow for bodies translating at small Reynolds number. Streamwise diffusion was assumed to be of the same order as streamwise convection, so that the second-derivative terms in x in the Navier–Stokes equations were retained. Oseen flow is therefore a solution to an equation which is elliptic, and its solutions are basically diffusive in character. This is in contrast to the high-Reynolds-number linearized theory proposed herewith. On effectively discarding the streamwise diffusion term at (18), the system becomes parabolic in x, and its solution is very different in character than that of Oseen. This becomes apparent below.

The integration in (18) dan be performed exactly using integral tables (Erdélyi *et al.* 1954). Taking care with the branches of the complex square roots so as to achieve vorticity convection downstream, the final integrated form of the vorticity Green function is

$$g(x,y;\xi,\eta) = \frac{1}{2\pi}\left(\frac{\pi\nu}{U}\right)^{\frac{1}{2}} \frac{\exp\left[-\frac{U}{4\nu}\frac{(y-n)^2}{x-\xi}\right]}{(x-\xi)^{\frac{1}{2}}} H(x-\xi). \tag{19}$$

5. Non-dimensionalization

With velocities non-dimensional on the stream speed U, distances non-dimensional on the body length L, and vorticity non-dimensional on U/L, the complete formulation of the proposed linearized theory, as applied to the 2-dimensional infinite-fluid case, is

$$\boldsymbol{V} = \boldsymbol{i} + \int_{l_b} \sigma \nabla G\,dl + \iint_S \omega \boldsymbol{k} \times \nabla G\,dS, \tag{20}$$

with

$$G = \frac{1}{2\pi}\ln\left[(x-\xi)^2 + (y-\eta)^2\right]^{\frac{1}{2}}; \tag{21}$$

$$\omega = \int_{l_b}\left(\omega\frac{\partial g}{\partial n} - \frac{\partial \omega}{\partial \eta}g\right)dl, \tag{22}$$

with

$$g = \frac{1}{2(\pi\,Re)^{\frac{1}{2}}} \frac{\exp\left[-\frac{Re}{4}\frac{(y-n)^2}{x-\xi}\right]}{(x-\xi)^{\frac{1}{2}}} H(x-\xi), \tag{23}$$

and with the boundary condition

$$\boldsymbol{V} = 0 \quad \text{on } l_b. \tag{24}$$

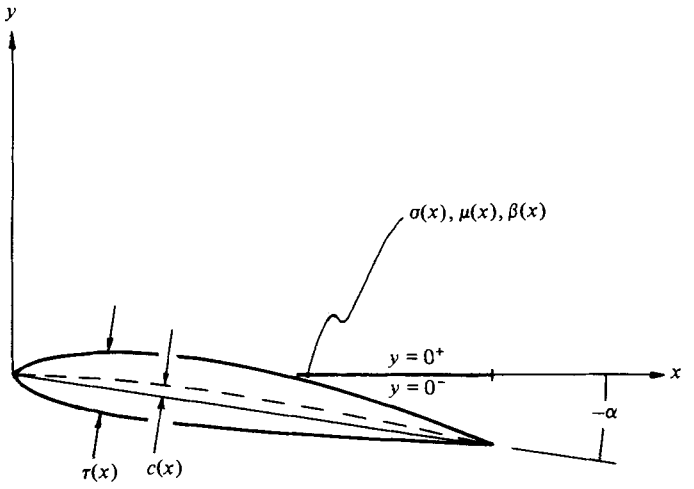

FIGURE 2. Thin-body geometry.

6. Application to thin bodies

The formulation (20)–(24) is now applied specifically to bodies that are thin enough so that the boundary condition can be satisfied approximately on the streamwise (x) axis, in the usual sense.

Employing the notation depicted on figure 2, the velocity and vorticity integrals (20) and (22) become

$$V(x,y) = \boldsymbol{i} + \int_{\xi=0}^{1} \sigma(\xi)\,\nabla G(x,y;\xi,0)\,\mathrm{d}\xi + \int_{\xi_1=-\infty}^{\infty}\int_{\eta_1=-\infty}^{\infty} \omega(\xi_1,\eta_1)\,\boldsymbol{k}\times\nabla G(x,y;\xi_1,\eta_1)\,\mathrm{d}\eta_1\,\mathrm{d}\xi_1, \quad (25)$$

$$\omega(x,y) = \int_{\xi=0}^{1}\left[-\mu(\xi)\frac{\partial}{\partial y} - \beta(\xi)\right] g(x,y;\xi,0)\,\mathrm{d}\xi. \quad (26)$$

The new unknown distributions μ and β in (26) appear on collapsing the body contour to the x-axis. They are respectively the 'vorticity doublet density'

$$\mu(x) = \omega(x,0^+) - \omega(x,0^-) \quad (27)$$

with axis in plus y, and the 'vorticity source density'

$$\beta(x) = \frac{\partial\omega}{\partial y}(x,0^+) - \frac{\partial\omega}{\partial y}(x,0^-). \quad (28)$$

On transferring from the body surface to the x-axis, the boundary condition (24) becomes, to first order,

$$V(x,0^\pm) = \left(\pm\frac{1}{2}\frac{\mathrm{d}\tau}{\mathrm{d}x} + \frac{\mathrm{d}c}{\mathrm{d}x} + \alpha\right)\boldsymbol{j} \quad (29)$$

$$\equiv v(x,0^\pm)\boldsymbol{j}.$$

Here $\tau(x)$, $c(x)$ and α are the thickness and camber distributions and the angle of attack of the thin body, as depicted on figure 2.

In applying the boundary condition (29) to determine the distributions σ, μ and

β in (25) and (26), (26) is substituted into (25) with G and g from (21) and (23). The resultant velocity components on $y = 0$, after exact integration in η_1, are

$$u(x,0^{\pm}) = 0 = 1+\frac{1}{2\pi}\int_{\xi=0}^{1}\frac{\sigma(\xi)}{x-\xi}\,\mathrm{d}\xi+\frac{1}{2}\frac{1}{(\pi Re)^{\frac{1}{2}}}\int_{\xi=0}^{x}\frac{\mu(\xi)}{(x-\xi)^{\frac{1}{2}}}\,\mathrm{d}\xi-\frac{1}{4}\frac{1}{(\pi Re)^{\frac{1}{2}}}$$
$$\times\int_{\xi=0}^{1}\mu(\xi)\int_{\xi_1=\xi}^{\infty}\frac{|x-\xi_1|}{(\xi_1-\xi)^{\frac{1}{2}}[(x-\xi)+(\xi_1-\xi)]^2}\,VF\left(\frac{|x-\xi_1|}{2}\left(\frac{Re}{\xi_1-\xi}\right)^{\frac{1}{2}}\right)\mathrm{d}\xi_1\,\mathrm{d}\xi, \tag{30}$$

$$v(x,0^{\pm}) = \pm\frac{1}{2}\frac{\mathrm{d}\tau}{\mathrm{d}x}+\frac{\mathrm{d}c}{\mathrm{d}x}+\alpha$$
$$= \pm\tfrac{1}{2}\sigma(x)-\frac{1}{4}\frac{1}{(\pi Re)^{\frac{1}{2}}}\int_{\xi=0}^{1}\beta(\xi)\int_{\xi_1=\xi}^{\infty}\frac{\operatorname{sgn}(x-\xi_1)}{(\xi_1-\xi)^{\frac{1}{2}}}\,VF\left(\frac{|x-\xi_1|}{2}\left(\frac{Re}{\xi_1-\xi}\right)^{\frac{1}{2}}\right)\mathrm{d}\xi_1\,\mathrm{d}\xi. \tag{31}$$

The function denoted VF in (30) and (31) is defined as

$$VF(a) \equiv \mathrm{e}^{a^2}\operatorname{erfc}(a), \tag{32}$$

with limiting values

$$\left.\begin{aligned}\lim_{a\to 0} VF(a) &= 1+O(a),\\ \lim_{a\to\infty} VF(a) &= O\left(\frac{1}{a}\right)\end{aligned}\right\} \tag{33}$$

Note from (30) and (31) that the tangential velocity $u(x,0^{\pm})$ does not depend on the vorticity source density β, while the normal velocity $v(v,0^{\pm})$ does not depend on the vorticity doublet density μ. This is a consequence of the odd characters of the integrands involving these functions in the η_1 integrations performed in (25).

The distributions, σ, μ and β are easily computable from (30) and (31). The velocity source density is determined first by matching the odd terms in (31). This gives $\sigma(x) = \mathrm{d}\tau/\mathrm{d}x$, which is the same familiar result from ideal-flow theory. $\mu(x)$ and $\beta(x)$ can then be calculated directly from (30) and the remaining (even) terms in (31); the integrals are numerically well behaved.

6.1. *High-Reynolds-number reductions*

Although the μ- and β-distributions can be computed numerically from (30) and (31) without difficulty, further simplifications result on focusing attention on the lowest-order contributions in the limit of high Reynolds number.

Considering the tangential velocity first, the first term involving $\mu(\xi)$ in (30) is the contribution from the singularity at $\xi_1 = x$, and it dominates the remainder integral as $Re\to\infty$, except perhaps for x very near zero. This can be seen by considering that as $Re\to\infty$ the function VF in (30) is $O(Re^{-\frac{1}{2}})$, by (33), except for x downstream of ξ and near ξ_1, where it is $O(1)$. But the factor on VF in the integrand is identically zero at $x = \xi_1$. In the interest of clarity, define a small parameter ϵ which is $O(Re^{-\frac{1}{2}})$ as $Re\to\infty$. Then, for $|x-\xi_1| = O(\epsilon)$ in (30), the remainder integral in (30) is $O(\epsilon\, Re^{-\frac{1}{2}}) = O(Re^{-1})$, as the function VF is no larger than $O(1)$. For $|x-\xi_1| = O(1)$, on the other hand, $VF = O(Re^{-\frac{1}{2}})$ by (33), with the result that the remainder integral is again $O(Re^{-1})$. Therefore the remainder integral term in (30) can be considered as no larger than $O(Re^{-1})$, and therefore of higher order relative to its principal part (the first μ-integral in (30)), which is $O(Re^{-\frac{1}{2}})$.

It should be noted that the first-order integral in (30) can be obtained directly by dropping the $\partial v/\partial x$ term in (3) and simply inverting $\omega = -\partial u/\partial y$ by direct integration in y.

In the high-Re limit, and excluding the region of x near zero, (30) can therefore be written

$$1+\frac{1}{2\pi}\int_{\xi=0}^{1}\frac{\sigma(\xi)}{x-\xi}\,\mathrm{d}\xi=-\frac{1}{2(\pi\,Re)^{\frac{1}{2}}}\int_{\xi=0}^{x}\frac{\mu(\xi)}{(x-\xi)^{\frac{1}{2}}}\,\mathrm{d}\xi. \tag{34}$$

This is an Abel integral equation on $\mu(x)$, whose inverse is well known. Denote the left-hand side of (34) by $u_{\mathrm{i}}(x,0)$, this is the potential-flow velocity tangent to the contour of the equivalent symmetric body of thickness $\tau(x)$. The inverse of (34) is

$$\mu(x)=-2\left(\frac{Re}{\pi}\right)^{\frac{1}{2}}\frac{\mathrm{d}}{\mathrm{d}x}\int_{\xi=0}^{x}\frac{u_{\mathrm{i}}(\xi,0)}{(x-\xi)^{\frac{1}{2}}}\,\mathrm{d}\xi. \tag{35}$$

Turning to the normal velocity (31), the ξ_1 integrand is maximum, just as with the tangential velocity, when x is downstream of ξ and $|x-\xi_1|$ is small. In this case VF in (31) is $O(1)$ as $Re\to\infty$. But, because of the sign change forced on the integrand at $\xi_1=x$, cancellation occurs in the integral for $|x-\xi_1|$ small. Denote this interval again by $|x-\xi_1|=O(\epsilon)$. The integration over the interval $|x-\xi_1|=O(\epsilon)$ in (31) can be taken as higher order in view of the cancellation. Then, for integration outside of this small interval, the argument of VF is large, and the function VF can be replaced by the leading term in its asymptotic expansion, i.e.

$$VF\left(\frac{|x-\xi_1|}{2}\left(\frac{Re}{\xi_1-\xi}\right)^{\frac{1}{2}}\right)\approx\frac{2}{(\pi\,Re)^{\frac{1}{2}}}\frac{1}{|x-\xi_1|}(\xi_1-\xi)^{\frac{1}{2}}\quad(|x-\xi_1|>\epsilon;\ Re\to\infty). \tag{36}$$

Substitution of (36) into (31), and allowing for complete limiting cancellation in $|x-\xi_1|=O(\epsilon)$, gives

$$v(x,0^{\pm})=\pm\tfrac{1}{2}\sigma(x)-\frac{1}{2\pi\,Re}\int_{\xi=0}^{1}\beta(\xi)\lim_{a\to\infty}\left\{\int_{\xi_1=\xi}^{a}\frac{\mathrm{d}\xi_1}{x-\xi_1}\right\}\mathrm{d}\xi. \tag{37}$$

Allowing that $\sigma(x)=\mathrm{d}\tau/\mathrm{d}x$ in (31), (37) takes the form

$$\frac{\mathrm{d}c}{\mathrm{d}x}+\alpha=-\frac{1}{2\pi\,Re}\int_{\xi=0}^{1}\beta(\xi)\ln|x-\xi|\,\mathrm{d}\xi-\lim_{a\to\infty}\ln a\int_{\xi=0}^{1}\beta(\xi)\,\mathrm{d}\xi. \tag{38}$$

But the integral $\int_{\xi=0}^{1}\beta(\xi)\,\mathrm{d}\xi$ in (38) is identically zero, as required by conservation of vorticity. That is, β has been identified as the vorticity source density; therefore its integral represents the net vorticity source strength. This must be zero because the vorticity-gradient field is divergenceless. Like fluid flow, vorticity flow must be conserved. Therefore.

$$\int_{\xi=0}^{1}\beta(\xi)\,\mathrm{d}\xi\equiv 0. \tag{39}$$

The integral equation (38) on $\beta(x)$ then takes the simple form

$$\frac{\mathrm{d}c}{\mathrm{d}x}+\alpha=-\frac{1}{2\pi\,Re}\int_{\xi=0}^{1}\beta(\xi)\ln|x-\xi|\,\mathrm{d}\xi. \tag{40}$$

It is enlightening at this point to integrate (40) by parts. Define

$$\gamma(x)\equiv\frac{1}{Re}\int_{\xi=0}^{x}\beta(\xi)\,\mathrm{d}\xi. \tag{41}$$

Then, on integration by parts, (40) becomes

$$\frac{\mathrm{d}c}{\mathrm{d}x}+\alpha=\frac{1}{2\pi}\int_{\xi=0}^{1}\frac{\gamma(\xi)}{\xi-x}\,\mathrm{d}\xi. \tag{42}$$

Equation (42) is immediately recognized as the airfoil integral equation from linearized ideal-flow theory; $\gamma(x)$ is the vortex density along the foil!

The proposed theory therefore supports the physical idea that the ideal flow is, in fact, the limiting state of the complete flow at infinite Reynolds number.

Note from (41) that the Kutta condition on the thin-foil problem, by the current theory, is, in reality, nothing more than a statement of conservation of vorticity, since

$$\gamma(1) = \frac{1}{Re}\int_{\xi=0}^{1} \beta(\xi)\,\mathrm{d}\xi = 0$$

by (39).

By (41), with $\beta(x)$ identified as the vorticity source density, $\gamma(x)$ is actually a vorticity doublet density, with axis tangent to the foil.

By definition, $\gamma(x)$ is the local jump in tangential velocity across the foil at x. From (41),

$$\beta(x) = Re\frac{\mathrm{d}\gamma(x)}{\mathrm{d}x}. \tag{43}$$

The vorticity souree density in the limit of infinite Reynolds number is therefore just the Reynolds number times the local chordwise rate of change of the tangential velocity jump across the foil.

The airfoil integral equation, whose solution produces $\beta(x)$ by (43), has the following well-known inverse:

$$\gamma(x) = \frac{2}{\pi}\left(\frac{1-x}{x}\right)^{\frac{1}{2}}\int_{\xi=0}^{1}\left(\frac{\mathrm{d}c}{\mathrm{d}\xi}+\alpha\right)\left(\frac{\xi}{1-\xi}\right)^{\frac{1}{2}}\frac{\mathrm{d}\xi}{x-\xi}. \tag{44}$$

6.2. *Circulation*

By definition, circulation is the space integral of vorticity:

$$\Gamma = \int_{x=-\infty}^{\infty}\int_{y=-\infty}^{\infty}\omega(x,y)\,\mathrm{d}y\,\mathrm{d}x. \tag{45}$$

$\omega(x,y)$ can be substituted from (26), with the vorticity Green function from (23). When this is done, the doublet density $\mu(x)$ from (26) disappears because its associated integrand is odd in y. Equation (45) becomes

$$\Gamma = -\frac{1}{(\pi Re)^{\frac{1}{2}}}\int_{\xi=0}^{1}\beta(\xi)\int_{x=-\infty}^{\infty}\frac{H(x-\xi)}{(x-\xi)^{\frac{1}{2}}}\int_{y=0}^{\infty}\exp\left(-\frac{Re}{4}\frac{y^2}{x-\xi}\right)\mathrm{d}y\,\mathrm{d}x\,\mathrm{d}\xi.$$

Integration in y produces

$$\Gamma = -\frac{1}{Re}\int_{\xi=0}^{1}\beta(\xi)\lim_{a\to\infty}\int_{x=\xi}^{a}\mathrm{d}x\,\mathrm{d}\xi$$

$$= \frac{1}{Re}\int_{\xi=0}^{1}\beta(\xi)\,\xi\,\mathrm{d}\xi - \frac{1}{Re}\lim_{a\to\infty} a\int_{\xi=0}^{1}\beta(\xi)\,\mathrm{d}\xi.$$

But the second integral is zero by (39), leaving

$$\Gamma = \frac{1}{Re}\int_{\xi=0}^{1}\beta(\xi)\,\xi\,\mathrm{d}\xi. \tag{46}$$

This integral can be integrated by parts to recover the conventional definition of circulation from the context of thin-foil theory. Using (41),

$$\Gamma = -\int_{\xi=0}^{1}\gamma(\xi)\,\mathrm{d}\xi. \tag{47}$$

6.3. *Surface shear stress*

The fluid shear stresses on the upper and lower surfaces of the thin body are of interest, in that negative surface shear stress is produced by backflow, and it therefore serves to define regions of flow separation.

By Stokes law the shear stress tangent to the body contour is the fluid-dynamical viscosity times the normal gradient of the fluid velocity. But, since the normal component of the velocity is identically zero on the contour, the normal velocity gradient is just the negative of the surface vorticity. For conditions satisfied on the axis of the thin body,

$$\tau(x, 0^{\pm}) = \mp \mu_0 \, \omega(x, 0^{\pm}),$$

where the constant μ_0 is the fluid-dynamical viscosity. In terms of the current non-dimensionalization,

$$\frac{\tau(x, 0^{\pm})}{\rho U^2} = \mp \frac{1}{Re} \omega(x, 0^{\pm}). \tag{48}$$

The surface vorticity is obtained from (26), with g from (23). Evaluating the integral on $y = 0^{\pm}$ gives

$$\omega(x, 0^{\pm}) = \pm \tfrac{1}{2} \mu(x) - \frac{1}{2} \frac{1}{(\pi Re)^{\frac{1}{2}}} \int_{\xi=0}^{x} \frac{\beta(\xi)}{(x-\xi)^{\frac{1}{2}}} \, \mathrm{d}\xi. \tag{49}$$

Therefore, once μ and β have been obtained from the integral-equation solutions, the predicted occurrence of flow separation can be simply assessed by way of (48) and (49).

7. Examples

7.1. *Flat plate with zero thickness and incidence*

The simplest case to which the theory can be applied is the zero-thickness flat plate oriented parallel to the stream.

From (31), or (44), the vorticity source strength $\beta(x)$ is zero for this case. The field vorticity is therefore given by (26) as

$$\omega(x, y) = -\int_{\xi=0}^{1} \mu(\xi) \frac{\partial}{\partial y} g(x, y; \xi, 0) \, \mathrm{d}\xi. \tag{50}$$

The vorticity doublet density μ is obtained from (35) with $\sigma(x) = 0$ in the surface ideal velocity $u_i(x, 0)$. Performing the integration and differentiation required by (35) gives

$$\mu(x) = -2 \left(\frac{Re}{\pi x} \right)^{\frac{1}{2}}. \tag{51}$$

A normalized surface shear stress from (48) and (49) is

$$\frac{\tau(x, 0^{\pm})}{\rho U^2} (\pi Re)^{\frac{1}{2}} \equiv \bar{\tau}(x, 0^{\pm}) = -\left(\frac{\pi}{Re} \right)^{\frac{1}{2}} \frac{\mu(x)}{2}. \tag{52}$$

Substituting (51),

$$\bar{\tau}(x, 0^{\pm}) = x^{-\frac{1}{2}}.$$

The shear stress is therefore positive and equal on both sides of the plate. Separation is predicted not to occur, which is most certainly the case.

The field vorticity produced by the plate is readily predicted from (50) and (51). Integration gives

$$\omega(x,y) = \begin{cases} -\left(\frac{Re}{\pi x}\right)^{\frac{1}{2}} \exp\left(-\frac{Re}{4}\frac{y^2}{x}\right) \operatorname{sgn}(y) & (0 < x \leqslant 1), \\ -\left(\frac{Re}{\pi x}\right)^{\frac{1}{2}} \exp\left(-\frac{Re}{4}\frac{y^2}{x}\right) \operatorname{erf}\left(\frac{y}{2}\left(\frac{Re}{x(x-1)}\right)^{\frac{1}{2}}\right) \operatorname{sgn}(y) & (x > 1). \end{cases} \tag{53}$$

Note that, unlike the prediction of boundary-layer theory (Schlichting 1968), the plate-surface vorticity by (53) is continuous from the plate surface into the wake $x \geqslant 1$, $y = 0$. For $x > 1$, $y = 0$, the error function is zero, giving zero vorticity along the axis, as is required. On the other hand, for $|y|$ arbitrarily small, as $x \to 1$ from downstream, erf $\to 1$ and

$$\omega(1, 0^{\pm}) \to \mp \left(\frac{Re}{\pi}\right)^{\frac{1}{2}}.$$

The vorticity at the end of the plate is therefore recovered on approaching the plate from the wake.

The velocity field can also be easily calculated on retaining the approximation

$$\omega \approx -\frac{\partial u}{\partial y}. \tag{54}$$

As previously discussed, this is equivalent to the high-Reynolds-number approximation employed at (30) to achieve the simplified $\mu(x)$ integral equation (34).

Integrating (54) in y, with ω from (53):

$$u(x,y) = \begin{cases} \operatorname{erf}\left(\frac{y}{2}\left(\frac{Re}{x}\right)^{\frac{1}{2}}\right) & (0 < x \leqslant 1), \\ 1 - \frac{1}{\pi}\int_{\xi=0}^{1} \frac{\exp\left(-\frac{Re}{4}\frac{y^2}{x-\xi}\right)}{(\xi(x-\xi))^{\frac{1}{2}}} \mathrm{d}\xi & (x > 1). \end{cases} \tag{55}$$

The evaluation of the last integral in (55) is not readily apparent. However, since $x > 1$, y can be set to zero in the integrand without difficulty to evaluate the velocity along the x-axis behind the plate. It is

$$u(x,0) = 1 - \frac{2}{\pi} \arctan \frac{1}{(x-1)^{\frac{1}{2}}} \quad (x > 1). \tag{56}$$

Here again, the wake velocity is continuous to the no-slip value of zero on approaching the plate end from the wake:

$$\lim_{x \to 1^+} u(x,0) = 1 - \frac{2}{\pi}\left(\frac{\pi}{2}\right) = 0.$$

By boundary-layer theory a singularity in $u(x,0)$ occurs at the plate trailing-edge stagnation point.

For large values of x behind the plate, $x \gg 1$ in (56), and the axial wake velocity takes the limiting form

$$u(x,0) = 1 - \frac{2}{\pi x^{\frac{1}{2}}}.$$

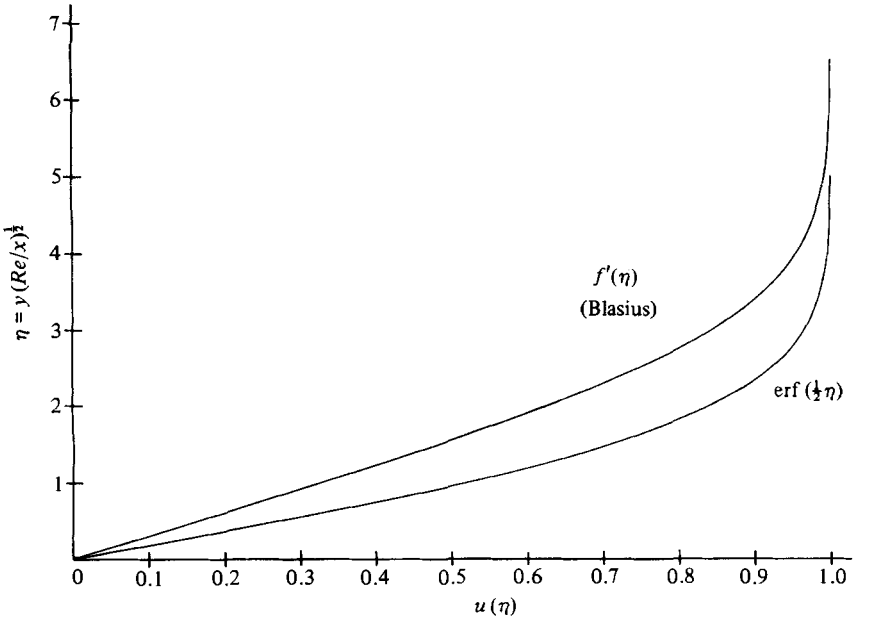

FIGURE 3. Flat-plate velocity profiles.

This compares with the asymptotic boundary-layer solution due to Goldstein (Schlichting 1968):

$$u(x,0) = 1 - \frac{0.664}{(\pi x)^{\frac{1}{2}}}.$$

Therefore, for any value of $x \gg 1$, the wake velocity defect is more severe by the current approximation than by that due to Goldstein.

The same tendency appears in the plate velocity profile by (55), compared to that of Blasius (Schlichting 1968). First denoting $\eta = y(Re/x)^{\frac{1}{2}}$, the plate boundary-layer profile from (55) is

$$u(x,y) = \operatorname{erf}(\tfrac{1}{2}\eta). \tag{57}$$

This is compared with the Blasius profile on figure 3.

The linear theory, by (57), predicts a 'fuller' velocity profile than does the Blasius boundary-layer solution, as shown on figure 3. This is no doubt due to the overestimate of vorticity convection near the plate surface, which is inherent in the current theory.

7.2. *More-general symmetric cases*

The symmetric flat plate is of limited interest since flow separation does not occur. For the symmetric case with thickness, the surface shear stress is still given by (52), but with $\mu(x)$ calculated more generally from (35) with $\sigma(x) \neq 0$.

The $u_i(x,0)$ in (35) has been defined as the potential-flow velocity over the surface of the symmetric body. It is zero at both $x = 0$ and $x = 1$, which positions correspond to the forward and after stagnation points respectively. This suggests a Fourier sine-series representation for u_i, in the form

$$u_i(x,0^{\pm}) = \sum_{n=1}^{\infty} A_n \sin n\pi x \quad (0 \leqslant x \leqslant 1).$$

Substitute this series into (35) and interchange the order of summation and integration:

$$\mu(x) = -2\left(\frac{Re}{\pi}\right)^{\frac{1}{2}} \sum_{n=1}^{\infty} A_n \frac{\mathrm{d}}{\mathrm{d}x} \int_{\xi=0}^{x} \frac{\sin n\pi\xi}{(x-\xi)^{\frac{1}{2}}} \mathrm{d}\xi.$$

Integration gives

$$\mu(x) = -2Re^{\frac{1}{2}} \sum_{n=1}^{\infty} A_n (2n\pi)^{\frac{1}{2}} [\cos(n\pi x) C_2(n\pi x) + \sin(n\pi x) S_2(n\pi x)]. \tag{58}$$

Here C_2 and S_2 are the Fresnel integrals.

For x near 1, the arguments of the Fresnel integrals can be considered as large; these functions asymptote to a value of $\frac{1}{2}$ for large argument. The position of the flow-separation points, corresponding to $\tau(x, 0^{\pm}) = 0$, from (52), can therefore be approximated from

$$\sum_{n=1}^{\infty} A_n n^{\frac{1}{2}} (\cos n\pi x + \sin n\pi x) = 0$$

or

$$\sum_{n=1}^{\infty} A_n n^{\frac{1}{2}} \cos(n\pi x - \tfrac{1}{4}\pi) = 0. \tag{59}$$

The simplest possible potential-flow distribution to which (59) can be applied is

$$u_i = A_1 \sin n\pi x. \tag{60}$$

For $A_1 = 2$, this corresponds to the ideal flow velocity over the surface of a circular cylinder, if x is measured along the circular contour. Now the circular cylinder is certainly not a thin body, and the subject formulation is therefore not truly applicable. The result is nevertheless interesting.

For $A_1 = 2; A_n = 0, n > 1$, in (59), the position of the separation points corresponds to

$$\cos(\pi x - \tfrac{1}{4}\pi) = 0$$

or

$$x = \tfrac{3}{4}.$$

This is a position angle on the circular cylinder of $\pm\frac{3}{4}\pi$, or $\pm 135°$. The Blasius series solution to the laminar boundary-layer equations predicts that separation occurs at 109°. According to Goldstein (1965), the position of the circular-cylinder separation point for high-Reynolds-number turbulent flow is difficult to estimate with exactness from experiments, but appears to fall between 122 and 130°.

The separation-point analysis by (59) was also performed on a 4:1 ellipse using 15 terms in the Fourier-series expansion for $u_i(x, 0)$. Separation was predicted at $x = 0.93$. Polhausen's method (Schlichting 1968), based on laminar boundary-layer theory, predicts a value of $x = 0.84$ as the position of the separation point on a 4:1 ellipse.

7.3. *Flat plat with non-zero thickness and incidence*

For a flat plate with angle of attack α, integration of (44), with $c(x) = 0$, gives the vortex density

$$\gamma(x) = 2\alpha \left(\frac{1-x}{x}\right)^{\frac{1}{2}}. \tag{61}$$

Then, by (43), the vorticity source density is

$$\beta(x) = Re\,\gamma'(x) = \frac{-\alpha\, Re}{(x^3(1-x))^{\frac{1}{2}}}. \tag{62}$$

For *zero* thickness, the vorticity normal doublet density $\mu(x)$ is the same as that previously developed for the zero-thickness flat plate at zero incidence, i.e. (51):

$$\mu(x) = -2\left(\frac{Re}{\pi x}\right)^{\frac{1}{2}}.$$

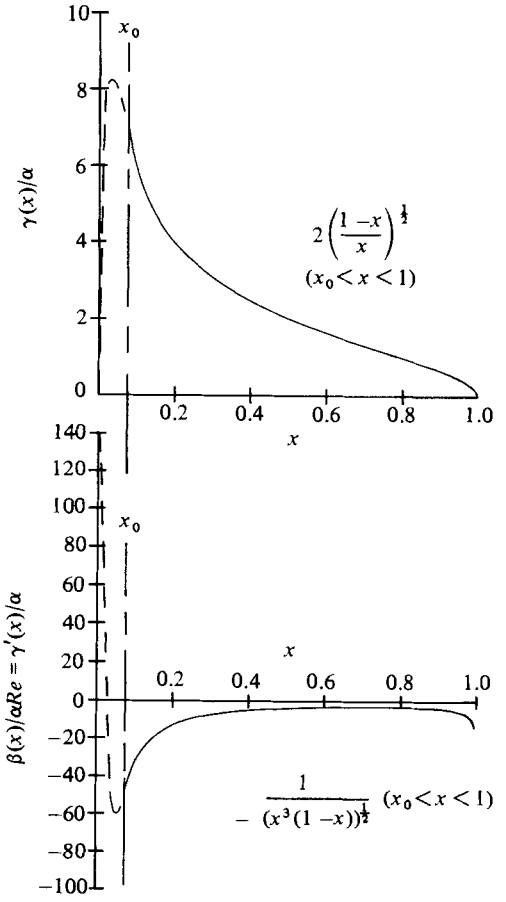

FIGURE 4. Flat plate with incidence, leading-edge characteristics.

The normalized surface shear stress, from (48), (49) and (52), is then

$$\bar{\tau}(x, 0^{\pm}) = \frac{1}{x^{\frac{1}{2}}} \pm \frac{1}{2} \int_{\xi=0}^{x} \frac{\gamma'(\xi)}{(x-\xi)^{\frac{1}{2}}} \mathrm{d}\xi. \tag{63}$$

An apparent difficulty exists at (63) because of the higher-order singularity in β at $x = 0$ implied by (62). Actually $\beta(x)$ must be finite at $x = 0$. Figure 4 is a sketch of the function $\gamma(x)$, by (61), as well as $\beta(x)$, (62), in the region $x_0 \leqslant x \leqslant 1$, $x_0 \to 0$. The necessary character of the functions into the origin is also indicated. The representations (61) and (62) do not include the vanishingly small region $0 \leqslant x < x_0$ indicated on figure 4. In this region the vortex density, by necessity, increases from zero at $x = 0$, peaks, and decreases to the inflexion point near x_0, whereafter it follows (61). However, in view of the γ' characteristic of figure 4, the details of the leading-edge behaviour should not be of great concern in the γ' integral of (63), as cancellation will obviously be occurring in the integration over the interval $0 \leqslant x < x_0$. Assuming that the integration in this small region is identically zero, the lower limit zero in the integral of (63) can be replaced by x_0. Here it is to be understood that x_0 is some small value, relative to x, which represents the approximate position of the inflexion point in the vortex density curve, or, equivalently, in the foil pressure jump characteristic.

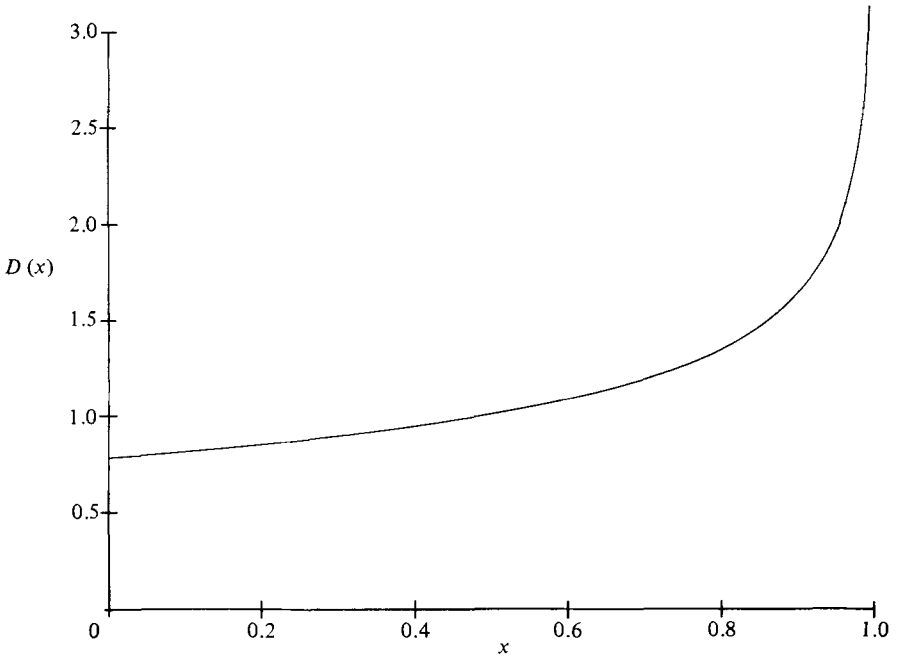

FIGURE 5. Elliptic integral $D(x) = [K(x)-E(x)]/x^2$.

Substitute $\gamma'(x)$ from (62) into (63) and integrate. The result is, after retaining the first-order terms for $x_0/x \ll 1$,

$$\bar{\tau}(x, 0^{\pm}) = \frac{1}{x^{\frac{1}{2}}}\left\{1 \pm \alpha\left[\frac{1}{x_0^{\frac{1}{2}}} + x^{\frac{1}{2}} D(x^{\frac{1}{2}})\right]\right\}. \tag{64}$$

Here

$$D(a) \equiv \frac{K(a)-E(a)}{a^2},$$

where K and E are the complete elliptic integrals of the first and second kinds. The limiting behaviour of D is

$$\lim_{a\to 0} D(a) = \tfrac{1}{4}\pi + O(a^2),$$

$$\lim_{a\to 1} D(a) = O[\ln(1-a^2)].$$

Figure 5 is a graph of the function $D(x)$ in (64).

For the suction side of the foil being positive y, as shown on figure 2, the angle of attack, α, in (64), has negative value. Therefore it is obvious from (64) that, from the fully attached flow at $\alpha = 0$, as the angle of attack increases to non-zero negative values the suction side of the foil separates. For $\alpha \neq 0$ a small value of x_0 can, in fact, always be selected such that the foil is fully separated for all $x \gg x_0$. The one disturbing aspect of (64) is that, on consideration of the characteristics of $D(x^{\frac{1}{2}})$, as angle of attack increases for fixed x_0, the separation point moves forward from the trailing edge; the accompaniment of leading-edge separation and reattachment is not predicted. Observations indicate that, with increasing angle of attack from zero, distinct regions of separation typically first appear at both the leading and trailing edges of thin foils. The reattachment point forward moves aft and the separation point aft moves forward until the two coalesce at complete separation of the suction surface.

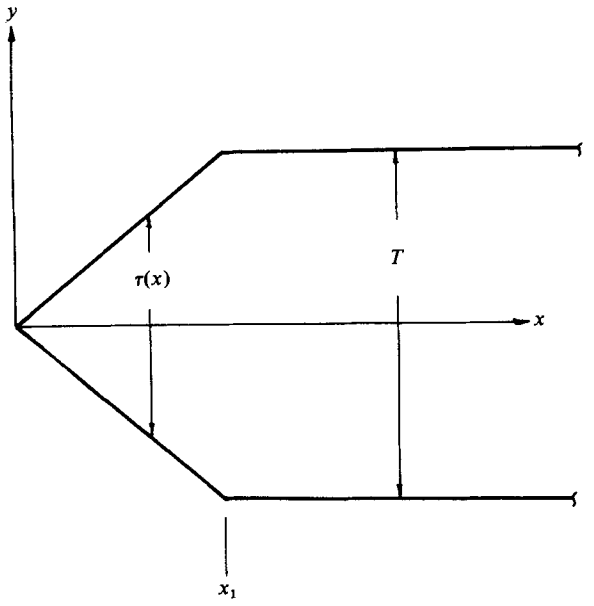

FIGURE 6. Flat-plate leading-edge thickness.

The most likely reason for the failure of (64) to predict leading-edge separation and reattachment appears to lie in the representation of $\mu(x)$ by (51). The shear stress due to $\mu(x)$, by (51), is the first term in (64). It is positive infinite at the leading edge, and therefore counteracts the negative leading-edge shear stress due to angle of attack, which is tending to produce separation. In reality, the high positive leading-edge shear stress associated with $\mu(x)$ should fall away more rapidly than $x^{-\frac{1}{2}}$ owing to the deceleration flow associated with finite-leading-edge thickness, which always exists.

The effects of thickness in $\mu(x)$ are included at (35) in the ideal-flow velocity

$$u_i(x,0) = 1+\frac{1}{2\pi}\int_{\xi=0}^{1}\frac{\sigma(\xi)}{x-\xi}\mathrm{d}\xi. \tag{65}$$

To allow for finite leading-edge thickness of the flat plate, represent the plate leading edge as the simple wedge shown on figure 6. Then, from figure 6,

$$\sigma(x) = \frac{\mathrm{d}\tau}{\mathrm{d}x} = \begin{cases} \dfrac{T}{x_1} & (0 \leqslant x \leqslant x_1), \\ 0 & (x > x_1). \end{cases}$$

Substitute $\sigma(x)$ into (65) with (65) then substituted into (35). After some manipulation

$$\mu(x) = -2\left(\frac{Re}{\pi}\right)^{\frac{1}{2}}\left[\frac{1}{x^{\frac{1}{2}}} - \frac{1}{2\pi}\frac{T}{x_1}\frac{\mathrm{d}}{\mathrm{d}x}\int_{\zeta=0}^{x_1}\frac{1}{(x-\xi)^{\frac{1}{2}}}\ln\frac{\left(\dfrac{x}{x-\zeta}\right)^{\frac{1}{2}}-1}{\left(\dfrac{x}{x-\zeta}\right)^{\frac{1}{2}}+1}\mathrm{d}\zeta\right]. \tag{66}$$

Performing the integration and differentiation required by (66), after retaining only lowest-order terms in the integrand for $x_1/x \ll 1$, produces

$$\mu(x) = -2\left(\frac{Re}{\pi x}\right)^{\frac{1}{2}}\left[1+\frac{T}{4\pi x}\left(1-\ln\frac{4x}{x_1}\right)\right]. \tag{67}$$

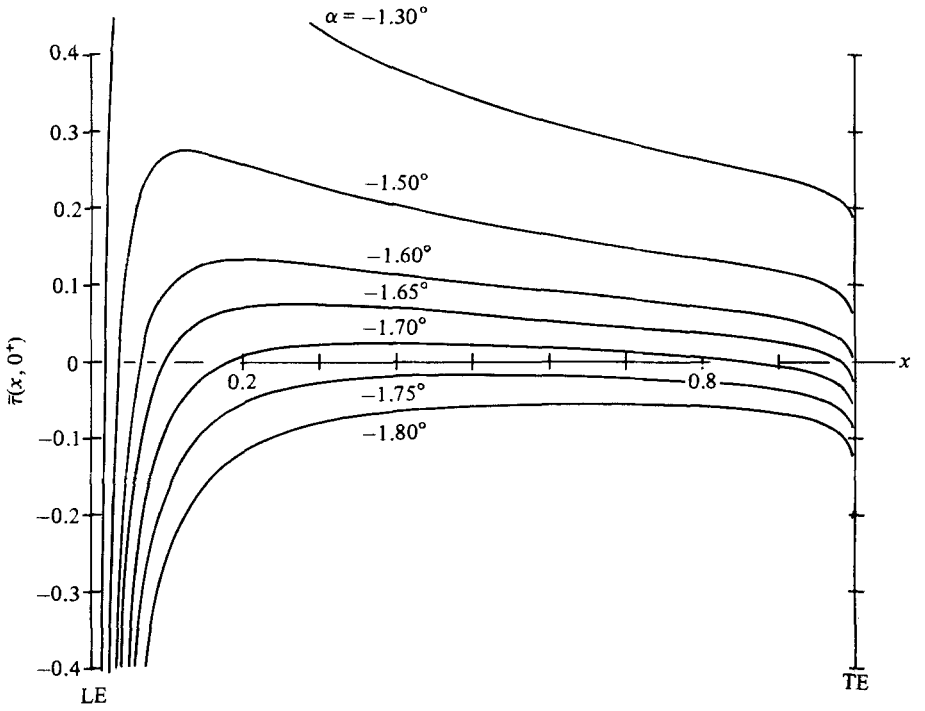

FIGURE 7. Flat plate with thickness and incidence; variation of suction-side shear stress with angle of attack.

Replacement of (51) by (67) in (64) gives the normalized surface shear stress on the flat plate with allowance for leading-edge thickness:

$$\bar{\tau}(x, 0^{\pm}) = \frac{1}{x^{\frac{1}{2}}}\left\{1 + \frac{T}{4\pi x}\left(1 - \ln\frac{4x}{x_1}\right) \pm \alpha\left[\frac{1}{x_0^{\frac{1}{2}}} + x^{\frac{1}{2}} D(x^{\frac{1}{2}})\right]\right\}. \tag{68}$$

The decelerating thickness flow from (66) produces the required behaviour in (68). For $x/x_1 > 1$ the terms multiplying T in (68) are collectively negative. This results in a more rapid decay of the positive component of the leading-edge shear stress away from $x = 0$, and thereby creates a more favourable environment for the occurrence of localized leading-edge separation.

Simple computations were performed using (68). The following values were arbitrarily selected for the parameters:

$$x_0 = x_1 = 0.001, \quad T = 0.02.$$

The results of the computations for $\bar{\tau}(x, 0^+)$ from (68) are shown on figure 7. Here the normalized shear stress on the suction surface is plotted versus distance along the flat plate from the leading edge, for values of angle of attack from $-1.3°$ to $-1.8°$.

First of all, figure 7 shows that the decelerating thickness flow at the leading edge does produce the localized leading-edge separation, as conjectured. Actually, (68) predicts that the leading-edge separation is imperceptible at zero angle of attack, existing essentially as an infinite discontinuity in the shear stress as x approaches x_1. On increasing angle of attack to negative values the leading-edge separation progresses after from the leading edge on the suction surface. At $-1.3°$ angle of attack for this example, the forward reattachment point is at approximately 2% of chord behind the leading edge.

A negative infinity in the trailing-edge shear stress also occurs; this is associated

with the angle-of-attack terms in (68), specifically $D(x^{\frac{1}{2}})$. However, figure 7 shows that, for the subject example, the after separation point has not moved perceptibly off the trailing edge up to approximately $-1.6°$ of angle of attack.

The leading-edge separation and reattachment therefore appear first in the figure 7 example. Beyond approximately $-1.6°$ incidence, suction-side trailing-edge separation begins to spread forward, accompanying the spread of leading-edge separation aft. The forward reattachment point and the aft separation point move toward one another beyond $-1.6°$. Coalescence occurs near the 40 % chord between $-1.7°$ and $-1.75°$ incidence. For higher angles of attack, the suction face of the foil is fully separated.

The behaviour predicted on figure 7 agrees, at least qualitatively, with observations (Goldstein 1965).

It is noteworthy that while increasing angle-of-attack, and lift, increases the degree of separation, by (68) and figure 7, the lift, to first order, is not affected by the degree of separation. The lift is from the vortex density according to ideal-flow theory, (44). This independence of lift on separation is a consequence of the first-order approximation on high Re employed at (34) and (36). If second-order terms are retained at (30) and (31), an influence of separation on lift will certainly appear.

Another important first-order effect obvious from (68) is that positions of separation and reattachment points are independent of Reynolds number; the separation- and reattachment-point positions correspond to $\bar{\tau}(x, 0^{\pm}) = 0$. The theory is predicting that while the thickness of the viscous flow tends to zero as $O(Re^{-\frac{1}{2}})$, separation and reattachment points asymptote to fixed positions on the body as infinite Re is approached. The character of the separation is therefore established in the lowest order. However, the separated flow is a subregion within the complete viscous field of the body. The thickness of the separation, versus its extent, therefore vanishes within the vanishing thickness of the entire viscous-flow domain as Re approaches the infinite limit. Again, retention of higher-order terms at (30) and (31) will impose a Reynolds-number dependency on the separation- and reattachment-point positions.

8. Far-field velocity

Return to the general linearized velocity field given by (25). If $\omega(x, y)$ is substituted from (26), with g from (23), and y is set to $O(1)$, retention of the lowest-order terms as $Re \to \infty$ gives

$$V(x,y) = i + \int_{\xi=0}^{1} \sigma(\xi)\, \nabla G(x,y;\xi,0)\, \mathrm{d}\xi - \int_{\xi=0}^{1} \kappa(\xi)\, \nabla G(x,y;\xi,0)\, \mathrm{d}\xi + \int_{\xi=0}^{1} \gamma(\xi)\, \mathbf{k} \times \nabla G(x,y;\xi,0)\, \mathrm{d}\xi. \quad (69)$$

The vortex density γ in (69) has been previously defined in terms of the vorticity source density β, according to (43), as

$$\gamma'(x) = \frac{\beta(x)}{Re}.$$

$\kappa(x)$ is similarly defined in (69) in terms of the vorticity normal doublet density μ as

$$\kappa(x) = \frac{\mu(x)}{Re}. \quad (70)$$

Note from (69) that while $\kappa(x)$ is actually a doublet density on vorticity, it contributes as a velocity source density with respect to the far-field flow. κ simply superimposes upon σ to form an effective source density allowing for sourcelike vorticity effects from the body near field. Denote this effective source density by

$$\sigma_e(x) = \sigma(x) - \kappa(x). \tag{71}$$

The far-field velocity is therefore of just the same form as the familiar result from thin-body ideal-flow theory:

$$\boldsymbol{V}(x,y) = \boldsymbol{i} + \int_{\xi=0}^{1} \sigma_e(\xi)\, \nabla G(x,y;\xi,0)\, d\xi + \int_{\xi=0}^{1} \gamma(\xi)\, \boldsymbol{k} \times \nabla G(x,y;\xi,0)\, d\xi. \tag{72}$$

Now reconsider the source density $\sigma_e(x)$. For a flat plate for which the thickness is zero, $\sigma_e = -\kappa$. But from (51), using (70), $\kappa(x)$ for the flat plate, at either zero or non-zero incidence, is, to first order,

$$\kappa(x) = -\frac{2}{(\pi\, Re\, x)^{\frac{1}{2}}}. \tag{73}$$

For a 2-dimensional body in ideal flow, the non-dimensional source density is the streamwise rate-of-change of body thickness. In this view, define an effective thickness of the viscous flow on both faces of the flat plate as $2\delta_e(x)$. This is consistent with the concepts of second-order boundary-layer theory. From (71) and (73), then,

$$\delta_e'(x) = \tfrac{1}{2}\sigma_e(x) = -\tfrac{1}{2}\kappa(x) = \frac{1}{(\pi\, Re\, x)^{\frac{1}{2}}}.$$

Integration gives

$$\delta_e(x) = 2\left(\frac{x}{\pi\, Re}\right)^{\frac{1}{2}}. \tag{74}$$

This effective thickness can be compared with the flat-plate boundary-layer thickness from figure 3. The boundary-layer thickness δ is conventionally defined at some x as the normal distance from the plate to the point at which the streamwise velocity has attained very nearly the free-stream value. From figure 3, the value of non-dimensional distance η at which the free stream is attained is approximately 5 by the Blasius boundary-layer solution; it is slightly less, approximately 4, by the subject linear theory. This implies a boundary-layer thickness according to Blasius of

$$\delta = 5\left(\frac{x}{Re}\right)^{\frac{1}{2}}, \tag{75}$$

or

$$\delta = 4\left(\frac{x}{Re}\right)^{\frac{1}{2}} \tag{76}$$

by the subject theory. In either case, comparison of (74) with (75) or (76) gives the predicted effective thickness of the rotational flow as seen from the far field as approximately one-quarter of the boundary-layer thickness.

Note, however, from (73), that κ in (69) is $O(Re^{-\frac{1}{2}})$, whereas the vortex density γ is $O(1)$. Therefore, the κ-term in (69) is actually higher order as $Re \to \infty$. That is, $\sigma_e \to \sigma$ by (71) as $Re \to \infty$. The first-order far-field velocity by the proposed unified theory is therefore predicted to be precisely that according to ideal-flow theory:

$$\boldsymbol{V} = \boldsymbol{i} + \int_{\xi=0}^{1} \sigma \nabla G\, d\xi + \int_{\xi=0}^{1} \gamma \boldsymbol{k} \times \nabla G\, d\xi.$$

9. Conclusion

When viewed from a broad perspective, one must conclude that the proposed theory demonstrates complete consistency with the physical idea that the ideal flow around a streamlined body represents the complete real flow, including any flow separation, in the limit as the body Reynolds number tends to infinity. The physical argument for the concept is that all viscous-flow effects, including separation, simply collapse into the infinitesimally thin body-surface vortex sheets as vorticity convection overwhelms vorticity diffusion in the infinite-Reynolds-number limit. Here a single vision scale, of fixed dimensions relative to body proportions, must be employed. This is versus the two separate vision scales fundamental to boundary-layer theory. When viewed on the single-vision scale, all viscous flow effects disappear completely from view onto the body surface as Re tends to infinity. The separated flow exists within the infinitesimally thin surface layer, but it has vanishing effect on the net lift and the far-field induced velocity as the infinite-Re limit is approached.

Consideration of this concept actually suggests an iteration scheme, where the first iterate is just the limiting ideal flow at infinite Reynolds number. The second iterate toward decreasing Reynolds number would be obtained, at least conceptually, by substituting the first-iterate velocity field into the differential equation on the vorticity Green function at (13), and computing a new solution. Back-substitution of the new solution into (13) would begin a new iteration, and so forth. The difficulty in the mechanics of this aside, the results demonstrated in the foregoing suggest that one could expect to obtain convergent steady laminar-flow solutions with separation. It is also interesting to postulate the possibilities of an extension of such a scheme for calculating unsteady laminar-flow effects, which become more important as Reynolds number is reduced.

Could it also be a possible approach to turbulence?!

REFERENCES

BATCHELOR, G. K. 1970 *An Introduction to Fluid Dynamics*. Cambridge University Press.

ERDELYI, A., MAGNUS, W., OBERHETTINGER, F. & TRICOMI, F. G. 1954 *Tables of Integral Transforms*. McGraw-Hill.

GOLDSTEIN, S. 1965 *Modern Developments in Fluid Dynamics*. Dover.

OSEEN, C. W. 1910 Über die stokessche Formel und über die verwandte Aufgabe in der Hydrodynamik. *Arch. Mat. Astron. Fys.* **6**, 29.

SCHLICHTING, H. 1968 *Boundary Layer Theory*, 6th edn. McGraw-Hill.